Numerical simulation of an optical chromatographic separator

Alex Terray, H.D. Ladouceur, Mark Hammond, Sean J. Hart*

Naval Research Laboratory, Chemistry Division, Bio/Analytical Chemistry, Code 6112, 4555 Overlook Ave. S.W., Washington, DC 20375
sean.hart@nrl.navy.mil

Abstract: Optical chromatography achieves microscale optical manipulation through the balance of optical and hydrodynamic forces on micron sized particles entrained in microfluidic flow traveling counter to the propagation of a mildly focused laser beam. The optical pressure force on a particle is specific to each particle's size, shape and refractive index. So far, these properties have been exploited in our lab to concentrate, purify and separate injected samples. But as this method advances into more complex optofluidic systems, a need to better predict behavior is necessary. Here, we present the development and experimental verification of a robust technique to simulate particle trajectories in our optical chromatographic device. We also show how this new tool can be used to gather better qualitative and quantitative understanding in a two component particle separation.

OCIS codes: (140) Lasers and laser optics; (140.7010) Trapping; (170.1420) Biology

References and links

1. A. Ashkin, "History of optical trapping and manipulation of small-neutral particle, atoms, and molecules," IEEE J. Sel. Top. Quantum Electron. **6**, 841-856 (2000).
2. D. G. Grier, "A revolution in optical manipulation," Nature **424**, 810-816 (2003).
3. S. J. Hart and A. V. Terray, "Refractive-index-driven separation of colloidal polymer particles using optical chromatography," Appl. Phys. Lett. **83**, 5316-5318 (2003).
4. S. J. Hart, A. V. Terray, and J. Arnold, "Particle separation and collection using an optical chromatographic filter," Appl. Phys. Lett. **91** (2007).
5. D. A. Ateya, J. S. Erickson, P. B. Howell Jr, L. R. Hilliard, J. P. Golden, and F. S. Ligler, "The good, the bad, and the tiny: A review of microflow cytometry," Anal. Bioanal. Chem. **391**, 1485-1498 (2008).
6. K. Dholakia, W. M. Lee, L. Paterson, M. P. MacDonald, R. McDonald, I. Andreev, P. Mthunzi, C. T. A. Brown, R. F. Marchington, and A. C. Riches, "Optical separation of cells on potential energy landscapes: Enhancement with dielectric tagging," IEEE J. Sel. Top. Quantum Electron. **13**, 1646-1654 (2007).
7. K. Ladavak, K. Kasza, and D. Grier, "Sorting by Periodic Potential Energy Landscapes: Optical Fractionation," Phys. Rev. E **70**, 010901 (2004).
8. T. Imasaka, "Optical chromatography. A new tool for separation of particles," Analusis **26**, M53-M55 (1998).
9. S. J. Hart, A. Terray, T. A. Leski, J. Arnold, and R. Stroud, "Discovery of a significant optical chromatographic difference between spores of Bacillus anthracis and its close relative, Bacillus thuringiensis," Anal. Chem. **78**, 3221-3225 (2006).
10. S. J. Hart, A. Terray, K. L. Kuhn, J. Arnold, and T. A. Leski, "Optical chromatography for biological separations," in *Proc. SPIE*(2004), pp. 35-47.
11. J. Makihara, T. Kaneta, and T. Imasaka, "Optical chromatography: Size determination by eluting particles," Talanta **48**, 551-557 (1999).
12. A. Terray, J. Arnold, S. D. Sundbeck, T. A. Leski, and S. J. Hart, "Preparative separations using optical chromatography," in *Proc. SPIE*(2007).
13. D. Bonessi, K. Bonin, and T. Walker, "Optical forces on particles of arbitrary shape and size," J. Opt. A: Pure Appl. Opt. **9**, S228-S234 (2007).
14. T. A. Nieminen, V. L. Y. Loke, A. B. Stilgoe, G. Knöner, A. M. Brańczyk, N. R. Heckenberg, and H. Rubinsztein-Dunlop, "Optical tweezers computational toolbox," J. Opt. A: Pure Appl. Opt. **9**, S196-S203 (2007).
15. R. C. Gauthier, "Computation of the optical trapping force using an FDTD based technique," Opt. Express **13**, 3707-3718 (2005).

#101972 - $15.00 USD Received 29 Sep 2008; revised 12 Dec 2008; accepted 14 Dec 2008; published 30 Jan 2009

Report Documentation Page

Form Approved
OMB No. 0704-0188

1. REPORT DATE	2. REPORT TYPE	3. DATES COVERED
2009		**00-00-2009 to 00-00-2009**

4. TITLE AND SUBTITLE	5a. CONTRACT NUMBER
Numerical simulation of an optical chromatographic separator	5b. GRANT NUMBER
	5c. PROGRAM ELEMENT NUMBER
6. AUTHOR(S)	5d. PROJECT NUMBER
	5e. TASK NUMBER
	5f. WORK UNIT NUMBER
7. PERFORMING ORGANIZATION NAME(S) AND ADDRESS(ES) **Naval Research Laboratory,Chemistry Division,Bio/Analytical Chemistry, Code 6112, 4555 Overlook Ave. S.W,Washington,DC,20375**	8. PERFORMING ORGANIZATION REPORT NUMBER
9. SPONSORING/MONITORING AGENCY NAME(S) AND ADDRESS(ES)	10. SPONSOR/MONITOR'S ACRONYM(S)
	11. SPONSOR/MONITOR'S REPORT NUMBER(S)

12. DISTRIBUTION/AVAILABILITY STATEMENT
Approved for public release; distribution unlimited

13. SUPPLEMENTARY NOTES

14. ABSTRACT

15. SUBJECT TERMS

16. SECURITY CLASSIFICATION OF:			17. LIMITATION OF ABSTRACT	18. NUMBER OF PAGES	19a. NAME OF RESPONSIBLE PERSON
a. REPORT	b. ABSTRACT	c. THIS PAGE			
unclassified	**unclassified**	**unclassified**	**Same as Report (SAR)**	**9**	

16. R. F. Marchington, M. Mazilu, S. Kuriakose, V. Garcés-Chávez, P. J. Reece, T. F. Krauss, M. Gu, and K. Dholakia, "Optical deflection and sorting of microparticles in a near-field optical geometry," Opt. Express **16**, 3712-3726 (2008).
17. R. C. Gauthier and M. Ashman, "Simulated dynamic behavior of single and multiple spheres in the trap region of focused laser beams," Appl. Opt. **37**, 6421-6431 (1998).
18. B. K. Sang, Y. Y. Sang, J. S. Hyung, and S. K. Sang, "Cross-type optical particle separation in a microchannel," Anal. Chem. **80**, 2628-2630 (2008).
19. Y. R. Chang, L. Hsu, and S. Chi, "Optical trapping of a spherically symmetric sphere in the ray-optics regime: A model for optical tweezers upon cells," Appl. Opt. **45**, 3885-3892 (2006).
20. P. A. Maia Neto and H. M. Nussenzveig, "Theory of optical tweezers," Europhys. Lett. **50**, 702-708 (2000).
21. T. Glatzel, C. Litterst, C. Cupelli, T. Lindemann, C. Moosmann, R. Niekrawietz, W. Streule, R. Zengerle, and P. Koltay, "Computational fluid dynamics (CFD) software tools for microfluidic applications - A case study," Comput. Fluids **37**, 218-235 (2008).
22. M. C. Kim, Z. Wang, R. H. W. Lam, and T. Thorsen, "Building a better cell trap: Applying Lagrangian modeling to the design of microfluidic devices for cell biology," J. Appl. Phys. **103** (2008).
23. *Fluent 6.3 User's Guide* (ANSYS, Inc., 2006).
24. S. B. Kim and S. S. Kim, "Radiation forces on spheres in loosely focused Gaussian beam: Ray-optics regime," J. Opt. Soc. Am. B **23**, 897-903 (2006).
25. *Fluent 6.3 UDF Manual* (ANSYS, Inc., 2006).
26. S. Ebert, K. Travis, B. Lincoln, and J. Guck, "Fluorescence ratio thermometry in a microfluidic dual-beam laser trap," Opt. Express **15**, 15493-15499 (2007).
27. T. Kaneta, Y. Ishidzu, N. Mishima, and T. Imasaka, "Theory of optical chromatography," Anal. Chem. **69**, 2701-2710 (1997).
28. A. Terray, J. Arnold, S. D. Sundbeck, T. A. Leski, and S. J. Hart, "Preparative Separations using Optical Chromatography," Proc. SPIE **6644**, 66441U (2007).

1. Introduction

With the advent of the laser and its continued growth as a tool for microscale optical manipulation[1], individual areas of research have developed into a widely investigated field that now encompasses research in diverse areas of physics, engineering, chemistry and biology. The term optical trapping has gained wide exposure and has become part of a growing body of research that deals with photon induced forces on microscopic particles[2]. This ability to interact with individual microscopic entities using a method akin to hand held control has allowed for, among other accomplishments, the separation and sorting of multicomponent colloidal samples[3, 4]. Individual particle characteristics such as size, refractive index, shape, and morphology dictate how and by what method these separations are achieved. To date, most have been accomplished by the exploitation of differences in the size and refractive index[3], while the remaining employ the creation of elegant microfluidic flow environments[5] and or novel transformations of the optical landscape[6, 7]. One such method is optical chromatography which involves the balance of forces on particles flowing in a microfluidic channel counter to the propagation of a mildly focused laser beam[8]. This method has been used to expose differences in the combined optofluidic effects to exquisitely fine resolutions to reveal differences in closely related biological samples[9], environmental samples[10] and various microspheres[3, 11]. More recently, modifications to the fluidic environment have allowed optical chromatography to not only determine optofluidic differences but to exploit these for the concentration, clean up and separation of biological and environmental samples[12]. Although this method has been very successful, further development of this and other methods would benefit greatly from more intimate knowledge and understanding of the forces a particle of interest is subject to while traveling through a specific optofluidic environment.

Theoretical and numerical treatments to calculate the optical and hydrodynamic forces on a particle of interest have been well documented for single particles in non dynamic situations under various optical and fluidic conditions [13-15]. Very few examples that dynamically model these interactions exist and those that do involve combinations of both the optical and hydrodynamic forces for only a very specific case or use approximations for one of the forces

#101972 - $15.00 USD Received 29 Sep 2008; revised 12 Dec 2008; accepted 14 Dec 2008; published 30 Jan 2009

[16-18]. Regardless of how these treatments are combined to describe forces on particles, the method to calculate individual hydrodynamic and optical forces are also distinct.

Current microscale optical methods attempt to solve for the optical forces in both the Rayleigh and the Mie regime and commonly use a ray-optics or an electromagnetic approach depending on the regime of interest, wavelength and particle size [19, 20]. Both approaches are successful at calculating the radiation force on a sphere exposed to a focused Gaussian beam. Fluidic methods in microfluidic systems use the Navier-Stokes equations to solve for the force due to hydrodynamic drag on spherical and non-spherical objects in low Reynolds number laminar flow [21, 22]. Each of these optical and fluidic approaches have been adapted to specific cases and can be used to predict how a particle of interest may behave, but only in very unique cases. A dynamic numerical method that fully calculates optical pressure, hydrodynamic drag forces and the resulting trajectories of spherical particles entrained in microfluidic flow has not been demonstrated and is desirable.

In this paper we demonstrate the numerical calculation of radiation pressure and hydrodynamic drag forces acting in concert on particles flowing through a complex optical fluidic environment. Using a commercial computational fluid dynamics (CFD) package, solutions to the force balance on particles as they progress from an injection through the optofluidic region were used to plot and predict particle trajectories. The ability to simulate an arbitrary injection of particles in a complex microfluidic design with the freedom to change conditions such as temperature, flow rate, laser power, number of beams, focusing optics, particle diameter, refractive index and geometry, make it an invaluable tool to aid in the design, development and analysis of many optofluidic separations. To test the accuracy of this method, initial simulations involving a pure injection of polystyrene (PS) microspheres were simulated and the results compared with experiment. The simulation method was then used to predict and investigate an optofluidic separation of PS and silica microspheres in our separation device.

2. Numerical simulation

All of the numeric calculations were performed using the commercial computational fluid dynamics package Fluent (Ansys, Inc., Canonsburg, PA, USA)[21]. The solution to the continuous phase was reached by numerically solving the Navier-Stokes equations for an incompressible Newtonian fluid via a finite element approach [23]. The calculation was based on the flowcell geometry, fluid properties and input boundary conditions. The particle trajectories were calculated using the Dynamic Particle Model (DPM) feature of Fluent by modeling a separate solid particle phase in a Lagrangian frame of reference[23]. The resulting data and particle trajectories were exported for analysis and visualization.

The velocity and pressure profiles for the continuous fluid phase were achieved using Fluent through several steps. A 3D model of our microfluidic device was drawn to scale in Solidworks (Solidworks Corporation, Concord, MA), Fig. 1, taking care to mimic the shape and dimensions of the actual device based on several collected measurements. This model was imported into Fluent's modeling and meshing software Gambit. The model was then meshed with grid spacing adequate to account for the smallest features. The resulting mesh was exported and opened in Fluent. The boundary conditions were chosen to reflect experimental observations and assumptions (20nl/min flow: pressure outlet, atmosphere, no-slip wall conditions, and water viscosity, 0.000852 kg/m*s at 27 ^{o}C. A pressure-based solver and a second-order upwind discretization scheme were used [23]. With a residual on continuity set to an absolute criterion of 1×10^{-6}, the inlet velocity was initialized and the problem was iterated to convergence. The final result yielded the expected laminar flow behavior. The converged solution was then used as the template to incorporate the dynamic particle model settings for particle trajectory calculations.

#101972 - $15.00 USD Received 29 Sep 2008; revised 12 Dec 2008; accepted 14 Dec 2008; published 30 Jan 2009

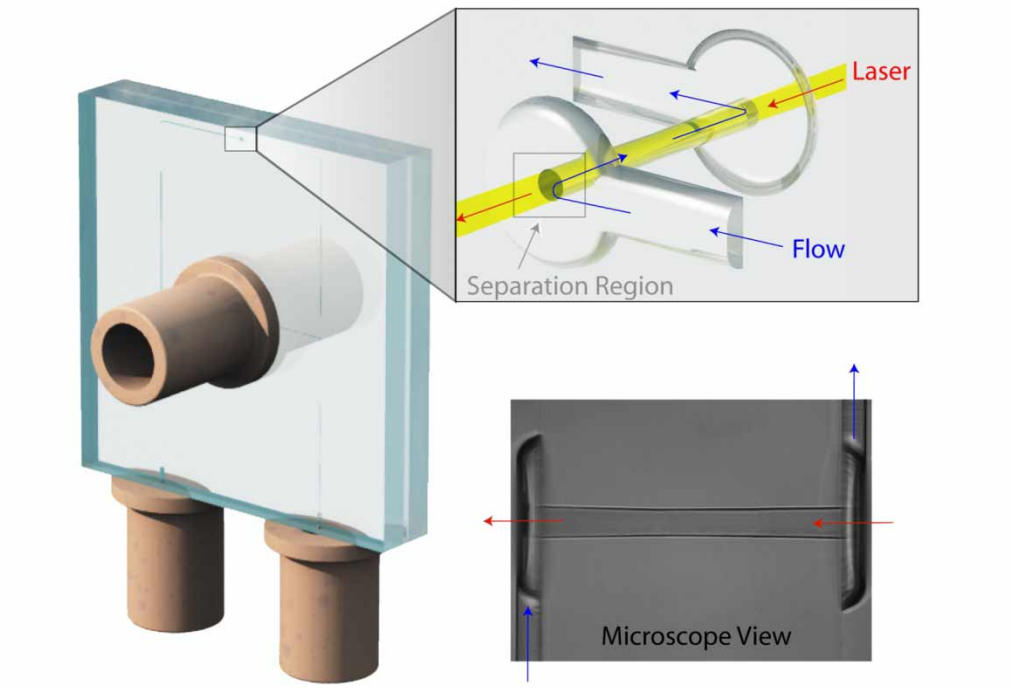

Fig. 1. An illustration of our three-layer fused silica optical chromatography separation device with fittings for injection, inlet and outlet connections. The exploded view shows the separation region with blue arrows indicating flow direction and red arrows indicating the propagation direction of the laser focused into the device. The laser focal point is positioned at the inlet wall with a diameter of about 36 microns and defocuses to fill the capillary at the opposite wall. The subset image shows a view of the separation region and capillary in the actual device through the 20x objective. The capillary is 500μm in length, with a slight taper of less than 1° to the center, and 55μm at each end.

Calculation of the discrete phase particle trajectories in Fluent involved the coupling of both the continuous phase and the discrete phase. Additionally, to complete the coupled optical and fluidic simulation, a custom force calculation in the discrete phase, was included from theory describing radiation pressure on a spherical particle in a loosely focused 1064nm Gaussian laser beam. The development of this theory, described elsewhere[24], is derived from a ray-optics method using a photon-stream approach and accurately describes the radiation force on a non-absorbing transparent sphere of greater refractive index than the solvent and whose size is larger than the wavelength of light and smaller than the beam diameter. The expressions and all auxiliary equations were inserted into a user defined function (UDF) using the C programming language as described in the Fluent UDF documentation [25]. This code was compiled and connected to Fluent allowing it to act as an additional body force in the particle force balance calculation. Including this radiation pressure calculation in the discreet phase particle model permitted us to fully simulate the three-dimensional trajectories of particles subject to several of the forces in our optofluidic system including inertial, hydrodynamic drag and radiation pressure. To compare the experimental system with the simulation, an accurate knowledge of the variables in the experiment is required.

3. Experimental

The experimental optical and fluidic system consisted of a continuous wave (CW) 1064nm

#101972 - $15.00 USD Received 29 Sep 2008; revised 12 Dec 2008; accepted 14 Dec 2008; published 30 Jan 2009

laser beam which was focused into a microfluidic flow cell, Fig. 1. Our highly configurable microfluidic device included a precisely calibrated flow and sample injection control system that allowed us to accurately determine and control the experimental conditions. Particle injections were made under known laser and fluidic conditions. The resulting particle trajectories were observed and the recorded data were analyzed for comparison to simulated results.

Our radiation source was a CW 0 to 8W 1064nm ytterbium fiber laser (IPG Photonics, Oxford, MA). The laser collimator head and 0.5 inch diameter near IR antireflection coated plano-convex 100mm focal length lens (Thorlabs, Newton, NJ) were mounted in a lens tube system (Thorlabs, Newton, NJ) which was attached to an x-y-z positioning stage (Newport Corporation, Irvine, CA). This allowed for precise and stable alignment of the focal point into the flow cell.

The geometric dimensions were determined by measuring calibrated images captured from several different views of the actual device. A laser focal diameter of 36 μm and position were measured from images collected of scatter from the laser passing through a suspension of glycogen using an infrared (IR) sensitive camera. The flow rate was determined from a commercial liquid mass flow meter (SLG-1430-025, Sensirion AG, Staefa, Switzerland). Laser power was measured before entering the flow device and decreased by 4% for standard losses through a flat plate to estimate the power in the device. The viscosity was determined from the temperature of distilled water in the device. The temperature was estimated by taking room temperature for the experiments (20^{o}C) and increasing the fluid temperature in the region containing the laser due to absorption of the 1064nm light. A very thorough treatment of absorption heating in a system very similar to ours was used to estimate this temperature increase[26]. By scaling this reported temperature rise to account for the fact that our beam was less focused and thus had a lower optical density in the intersecting laser and fluid volumes, while also considering that in both cases the total power was about 2W, we arrived at a value of 7^{o}C. This temperature rise is about half that observed in the referenced work due to this difference in the optical density. With this estimate, a final fluid temperature of 27^{o}C in the separation region where the laser passes through the device was used. To simplify the simulation, this temperature was used to set the viscosity of the fluid throughout the system.

Our microfluidic device was connected to a 5-axis positioner (New Focus, San Jose, CA) for alignment with the laser. The flowcell was fabricated from three fused silica plates etched and machined such that the resulting final device effectively performed as a single piece of fused silica in which our 3D microfluidic channel structure was contained. The one inch square 2mm thick front and back plates were wet etched resulting in a pattern of channels 120μm wide and 40μm deep which intersected machined 350 μm thru holes at the end points. The 500μm thick center plate had an etched separation channel about 50 microns in diameter penetrating completely through the plate (Translume Inc., Ann Arbor, MI). After precise alignment and bonding, fittings and 100 micron inner diameter Teflon tubing (Upchurch Scientific, Inc., Oak Harbor, WA) were attached to the flowcell for inlet, outlet and injection connections.

The fluid control system consisted of a pneumatically controlled reservoir involving very precise pressure control over a 20ml volume of pure water. The liquid volume was connected to tubing resulting in pulseless, stable and reproducible fluid flow. Computer control via an electronic pressure controller (OEM-EP, Parker Hannifin, Hollis, NH) allowed for rapid interactive manipulation of the pressure and thus flow rate. The complete system involved connecting the inlet and outlet tubing each to a separate reservoir. The dual reservoir system completely isolated the flow system increasing the stability and added the ability to control flow direction. Flow direction and flow rate were precisely measured to a resolution of 0.5nl/min using the calibrated commercial liquid mass flow meter. Sample injections were made using a syringe pump (NE-1000, New Era Pump Systems Inc, Farmingdale, NY)

#101972 - $15.00 USD Received 29 Sep 2008; revised 12 Dec 2008; accepted 14 Dec 2008; published 30 Jan 2009

containing a 10µl syringe (Hamilton Company, Reno, NV) connected to the injection tubing. Diluted samples of PS and Si microspheres with diameters of 1.9µm and 1.0µm respectively (Polysciences, Inc., Warrington, PA) were used in all of the experiments. The efficiency of optical pressure transfer (Q) for both spheres at our wavelength was 0.129 and 0.036 respectively [27].

Image data were collected from a CCD camera (Microfire, Olympus America Inc., Center Valley, PA) connected to compact microscope optics (InfiniTube, Infinity Photo-Optical, Boulder, CO) and a 20x objective (Olympus America Inc., Center Valley, PA). The image data were recorded at a frame rate of 2Hz and analyzed frame by frame using Image Pro Plus (Version 6.2, Media Cybernetics Inc., Silver Spring, MD). Particles were tracked manually rather than using background removal and contrast thresholding to remove any errors in particle identification while passing through a region in the flow cell that partially obscured the view of the particle.

4. Results

To test the accuracy of the simulation, several injections were made at flow rates ranging from 5 to 20nl/min using a pure dilute sample of 1.9µm PS microspheres and compared to the results of the corresponding simulation. For the experiment, particles were injected to saturate the flow system. The desired flow rate was set and the laser operated at a power of 2W. The result was a dynamic situation where particles entrained in the laminar flow, entered the separation region (Fig. 1, exploded view) and were subjected to the forces from the laser as flow entered the capillary and laser path. As an initial position for particle tracking, we chose an arbitrary point about 9µm from the channel edge slightly upstream from the separation region, Fig. 2. Particles that passed through this region and were clearly in focus (lying in the same focal position) were individually tracked as they passed into the region of the device where the laser was centered. The maximum distance the tracked particle entered the capillary, termed the entrance distance, was measured from the captured images.

For three separate injections and several individual particle tracks per injection a statistically significant number of entrance distances were compiled for each of six different flow rates ranging from 5 to 20nl/min. The results are shown in Fig. 3. It is clear that even though the simulated values slightly underestimated the experimental results, the simulated values are in good agreement with the experiment. One can see that the particle entrance distance had a maximum at 20nl/min and decreased as the flow was lowered. At a flow rate of 10nl/min and below, the fluidic drag forces were not enough to drive particles into the capillary against the opposing optical pressure force. Particles tracked a distance greater than 9µm from the wall were also completely diverted from the inlet, but particles passing less than 9µm continued to have a measurable entrance distance at 10 nl/min. This distance was reduced and eventually approached zero as flow decreased. Effectively, by changing the flow rate, the fraction of particles entering the separation region could be precisely manipulated.

With good agreement of our model to experiment, we chose to simulate the two component separation of 1.9µm PS and 1.0µm silica microspheres. In previous work, we have observed this separation in a related device under different flow conditions and with the laser focused more toward the center of the capillary [28]. To investigate a separation using

#101972 - $15.00 USD Received 29 Sep 2008; revised 12 Dec 2008; accepted 14 Dec 2008; published 30 Jan 2009

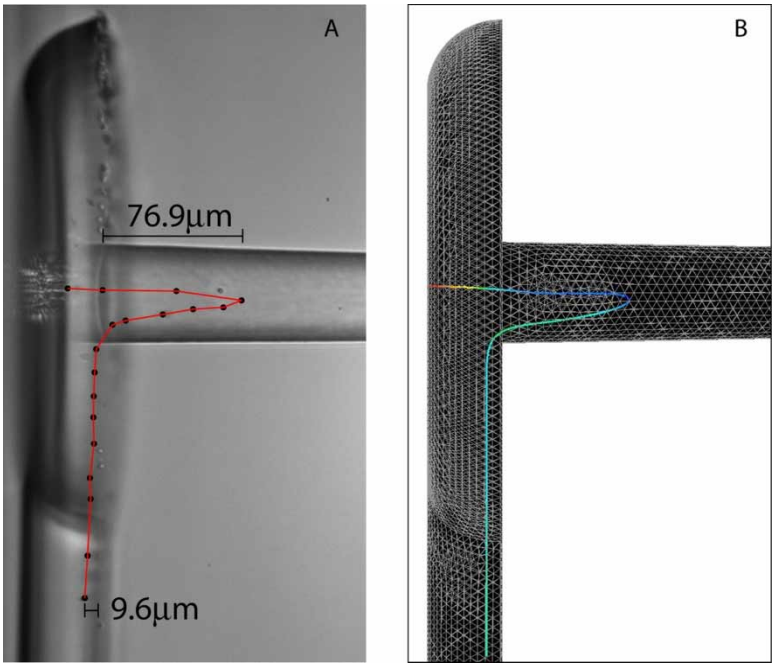

Fig. 2. Trajectory for a single 1.9µm PS particle at 20nl/min flow and 2W laser power (1.9W in the channel). (a) Experimental track from an image series collected at 2Hz (Media 1). The initial position from the wall and the maximum particle entrance distance are indicated. (b) Simulated trajectory using the experimental conditions with a resulting entrance depth of 83µm.

this method, we simulated pure injections of each component under identical conditions. To account for particle positions anywhere in the channel we created an injection consisting of evenly spaced particles occupying positions from wall to wall or the entire depth of the etched entrance channel. These particles were also centered in the etch channel as it was observed that an injection completely filling the entrance channel was not required to get a representative view of the particle retention. We positioned the injection slightly upstream and used the simulation to generate trajectories for each particle. The resulting trajectory plots for both pure injections are shown in Fig. 4. From these plots it is clear that the PS injection would be completely retained and only a small amount of the silica injection would be retained under these conditions. The simulation gives 100% retention for PS and 19% for silica. This represents a reasonable first pass fractionation of this sample and tells us that under our current conditions a small contamination of silica in the concentrated band of PS particles is to be expected. As this example shows, the ability to simulate provides for us a tool that will allow us to quickly and quantitatively predict, tune and better understand desired separations. Several simulations can also be quickly processed for multiple conditions and/or designs to obtain quantitative estimates of performance.

#101972 - $15.00 USD Received 29 Sep 2008; revised 12 Dec 2008; accepted 14 Dec 2008; published 30 Jan 2009

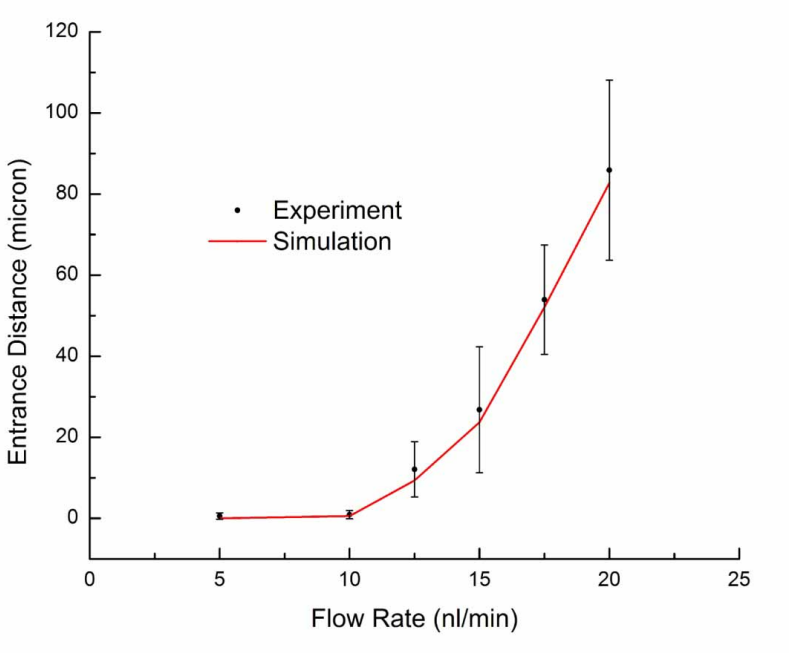

Fig. 3. Plot of flow rate and particle entrance distance for six different flow rates ranging from 5 to 20nl/min. The black circles are the average experimental values and standard deviation. The red line connects simulated values calculated under the same conditions at each experimental flow rate.

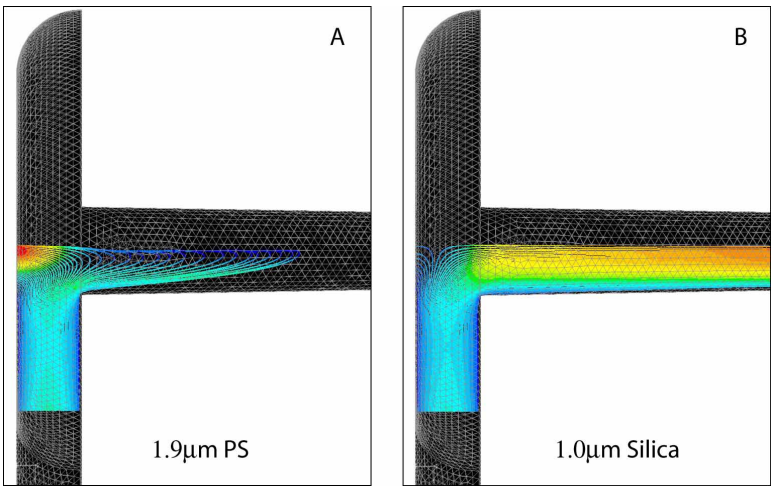

Fig. 4. Trajectories for simulated pure injections of (a) 1.9µm PS and (b) 1.0µm silica at a power of 1.9W (in the channel) and 20nl/min flow. The trajectories clearly illustrate that the PS particles are retained much more than the Si particles. Accompanying videos show the time progression of particles through the simulation and give a more dynamic feel to the simulation for these results (Media 2).

#101972 - $15.00 USD Received 29 Sep 2008; revised 12 Dec 2008; accepted 14 Dec 2008; published 30 Jan 2009

5. Conclusions

We have developed and experimentally verified a robust simulation technique using Fluent to predict particle trajectories in our optical chromatographic microfluidic separation device. Because this technique relies on Fluent, a well developed commercial CDF product, a wide variety of different and complex microfluidic systems incorporating one or more lasers can be readily simulated and compared with experimental data. In our lab, simulation of single and multicomponent injections has and will continue to be an asset for optimizing future separations.

Acknowledgments

The authors would like to acknowledge the Naval Research Laboratory (NRL) and the Defense Threat Reduction Agency (DTRA) for support of this research. The authors would also like to thank Dr. Ramagopal Ananth (NRL), Mr. Richard Stroman (NRL), Dr. Benjamin Gould (ASEE Postdoctoral Fellow) and Dr. Carl I. D. Newman (Strategic Analysis, Inc.) for in-depth discussions related to the manuscript.

#101972 - $15.00 USD Received 29 Sep 2008; revised 12 Dec 2008; accepted 14 Dec 2008; published 30 Jan 2009